Reviews

The nature and energy characteristics of intramolecular hydrogen bonds in crystals

K. A. Lyssenko and M. Yu. Antipin*

A. N. Nesmeyanov Institute of Organoelement Compounds, Russian Academy of Sciences, 28 ul. Vavilova, 119991 Moscow, Russian Federation. Fax: +7 (495) 135 6549. E-mail: kostya@xlab.ineos.ac.ru

The review concerns the results of systematic X-ray diffraction studies of the electron density distribution in the crystals of compounds with strong intramolecular hydrogen bonds N—H...O, O—H...O, O—H...N, and N—H...S. The advantages of the topological analysis of the electron density distribution function in the analysis of the nature and estimation of the H-bond energies directly from experimental data are discussed.

Key words: X-ray diffraction studies, quantum chemical calculations, topological analysis, electron density distribution function, intramolecular hydrogen bond N—H...O, O—H...O, O—H...N, and N—H...S, proton transfer in crystals.

The nature, energy characteristics, and the role of hydrogen bonding in supramolecular association and self-assembly of molecules in crystals have been the subject of so intensive research that it is impossible to summarize the available material on the subject. For instance, in a recently published review[1] dedicated solely to water trimer studies the bibliography includes a total of 271 references.

Research on intramolecular hydrogen bonds, especially the H-bonds stabilized through delocalization of the π-electron density (so-called resonance assisted H-bonds, RAHB),[2,3] has been carried out with at least comparable intensity. In contrast to the studies of intermolecular interactions, intramolecular H-bonds are more often analyzed using geometric parameters of the molecules including data of X-ray diffraction studies. This is the most widely used approach. Indeed, the energies of intermolecular H-bonds can be estimated using the energies of noninteracting molecules as references, but there are no such references when considering any intramolecular interactions. Clearly, the energy difference between two conformers, **A** and **B**, includes the energy of the H-bond, but cannot serve as a measure of the bond strength.

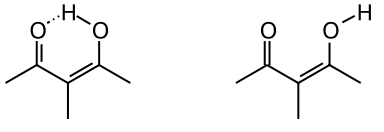

A **B**

Published in Russian in *Izvestiya Akademii Nauk. Seriya Khimicheskaya,* No. 1, pp. 1—14, January, 2006.

1066-5285/06/5501-0001

The energies of intramolecular H-bonds are most often estimated using the X...Y distance between the proton donor and proton acceptor. Usually, the term "strong hydrogen bond X—H...Y" implies that the X...Y distance is shorter than the sum of the van der Waals radii.[4] For instance, the limiting values of the lengths of strong hydrogen bonds O—H...O, N—H...O (O—H...N), and N—H...S are 2.58, 2.78, and 3.08 Å, respectively.[5] However, it is clear that the use of this parameter for comparing the energies of the H-bonds formed by different proton donors and acceptors is impossible.

Information on the type and strength of an H-bond can also be obtained by analyzing the bond length distribution in the H-bonded ring. This approach was most widely used in the studies of β-diketone enols.[6—11] In order to assess the type and evaluate the strength of H-bonds, it was proposed to use the differences between the C=O and C—OH bond lengths ($q_1 = d_1 - d_4$) and between the C—C and C=C bond lengths ($q_2 = d_2 - d_3$). Indeed, a good correlation between the parameter $Q = q_1 + q_2$ and the O...O distance was obtained[6,7] for a small set of structural data (20 structures). However, this correlation becomes invalid as the number of structures increases.[12]

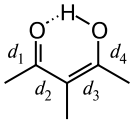

In addition, both intermolecular and intramolecular interactions can be unambiguously revealed by performing the topological analysis of the electron density distribution function ρ(**r**) in the framework of the "Atoms in molecule" (AM) theory using the data of X-ray diffraction studies.[13] Until recently, the topological analysis of the ρ(**r**) function served to obtain the electron density, electron density Laplacian, and bond ellipticity values, whereas calculations of other topological parameters, especially the kinetic, potential, and electron energy densities were impossible.

Indeed, calculations of the kinetic and potential energy densities require wave functions, which fact rules out the possibility of evaluating these parameters from experimental data. At the same time the kinetic energy density $g(\mathbf{r})$, as a function of ρ(**r**) and its derivatives, can be approximately described[14—18] in the framework of the so-called gradient expansion[19]:

$$g(\mathbf{r}) = \frac{3}{10}(3\pi^2)\rho(\mathbf{r})^{5/3} + \frac{1}{72}[\nabla\rho(\mathbf{r})]^2/\rho(\mathbf{r}) + \frac{1}{6}\nabla^2\rho(\mathbf{r}), \quad (1)$$

from which with allowance for the local virial theorem one gets

$$-L(\mathbf{r}) = (1/4)\nabla^2(\mathbf{r}) = v(\mathbf{r}) + g(\mathbf{r})$$

and the expressions for the potential and electron energy densities are as follows

$$v(\mathbf{r}) = -\frac{3}{5}(3\pi^2)\rho(\mathbf{r})^{5/3} - \frac{1}{36}[\nabla\rho(\mathbf{r})]^2/\rho(\mathbf{r}) - \frac{1}{12}\nabla^2\rho(\mathbf{r}), \quad (2)$$

$$h_e(\mathbf{r}) = -\frac{3}{10}(3\pi^2)\rho(\mathbf{r})^{5/3} - \frac{1}{72}[\nabla\rho(\mathbf{r})]^2/\rho(\mathbf{r}) + \frac{1}{12}\nabla^2\rho(\mathbf{r}). \quad (3)$$

Application of this approximation to the analysis of various systems showed that the best correspondence between the $g(\mathbf{r})$ values obtained using Eq. (1) and from the density matrix is obtained at long distances from the atomic nucleus and mainly for the closed-shell interactions, for which the difference is ~5% (*cf.* at least 20% for covalent bonds, see Refs 14—20).

In turn, the possibility of estimating the $g(\mathbf{r})$ values from experimental data made it possible to analyze the experimental electron pair localization functions (ELF)[21] and the local orbital locator (LOL)[22] using a recently proposed approach.

The greatest interest in the gradient expansion (1) is due to the possibility of estimating the contact energy based on the $v(\mathbf{r})$ values at the (3, −1) critical point. The results of analysis of 83 X—H...O contacts available from the literature showed that this approximation allows one not only to obtain semiquantitative estimates of the contributions to the local energy density but also to relate them to the energy of the contact (E_{cont}) and to energies of other weak specific interactions.[15,16] For instance, in the framework of this approach it was shown[15] that the E_{cont} values correlate with the potential energy density at the (3, −1) critical point

$$E_{cont}\ (\text{kcal mol}^{-1}) = 313.36 \cdot v(\mathbf{r})\ (\text{a.u.}). \quad (4)$$

This allows the X-ray diffraction methods to be used not only for elucidating the character of the atom-atom interactions but also estimating their energies in the crystal.

Therefore, in this work we will (i) show the potentialities of modern high-precision X-ray diffraction techniques in studies on the nature of H-bonds and evaluation of their energies and (ii) discuss the problems that are posed when using geometric parameters, especially in the framework of the RAHB theory.

For instance, according to the RAHB concept, the tautomer having a stronger H-bond should correspond to the energy minimum, because in this case the H-bonded ring better resembles the "aromatic" ring.[6,7] Consider now to which extent does this assumption agree with the experimental data and whether equalization of the bond lengths in the H-bonded ring does correspond to delocalization of the π-electron density.

Quite a representative example is provided by a study of 3-acetyl-4-hydroxycoumarine (**1**). According to quantum chemical and multitemperature (100—353 K) X-ray diffraction studies of compound **1**, the energy minimum was obtained[12] for the tautomer with the longer O...O distance (Scheme 1).

Scheme 1

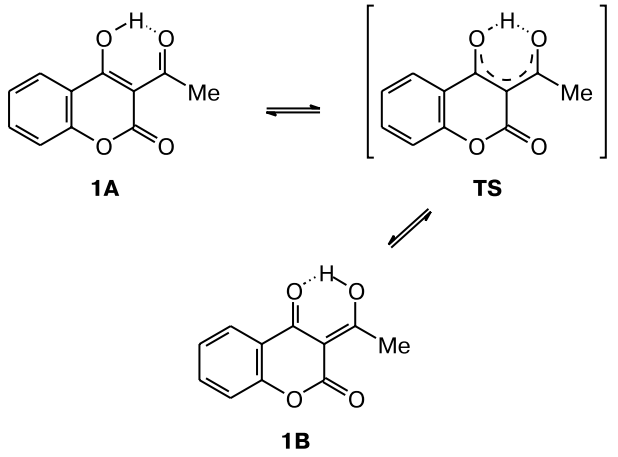

According to B3LYP/6-31G(d,p) calculations, the barrier to intramolecular proton transfer along the O...O line is 2.86 (**1A**/**TS**) and 1.97 kcal mol^{-1} (**TS**/**1B**) and the hydrogen bond length is 2.447 Å (*cf.* experimental values of 2.442(1) Å for **1A**, 2.360 Å for **TS**, and 2.431 Å for **1B**).

A similar picture was also obtained for benzoylacetone. Here, the energetically more favorable tautomer (energy difference between tautomers is 0.74 kcal mol^{-1}) is also characterized by higher vibrational frequency ν(OH) and longer O...O distance (see Ref. 23).

It should be noted that if for benzoylacetone[23] and 3-acetyl-4-hydroxycoumarine (**1**)[12] the O...O distances in tautomers differ insignificantly (by 0.01 Å), for 3*Z*,5*E*-6-(4-chlorophenyl)-1,1,1-trifluoro-4-hydroxyhexa-3,5-dien-2-one (**2**, Scheme 2) the effect is more pronounced.[24] PBEPBE/DGDZVP2/DGA1 quantum chemical calculations of two tautomers of **2** showed that tautomer **2A** is 1.78 kcal mol^{-1} more stable than tautomer **2B**, although the O—H...O intramolecular bond in **2A** is much weaker than in **2B** (O...O 2.510 *vs.* 2.430 Å, respectively). Interestingly, the *Q* value for **2A** (0.074 Å) is somewhat smaller than for **2B** (0.090 Å); therefore, strengthening of the

Scheme 2

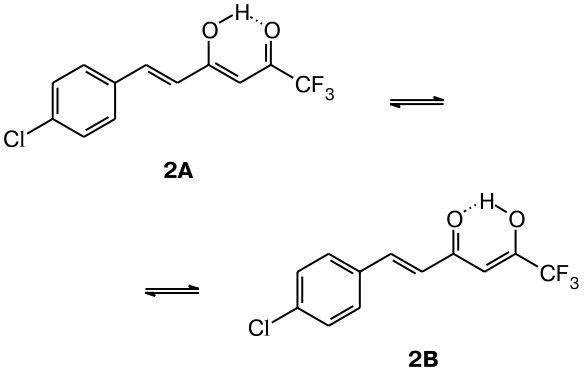

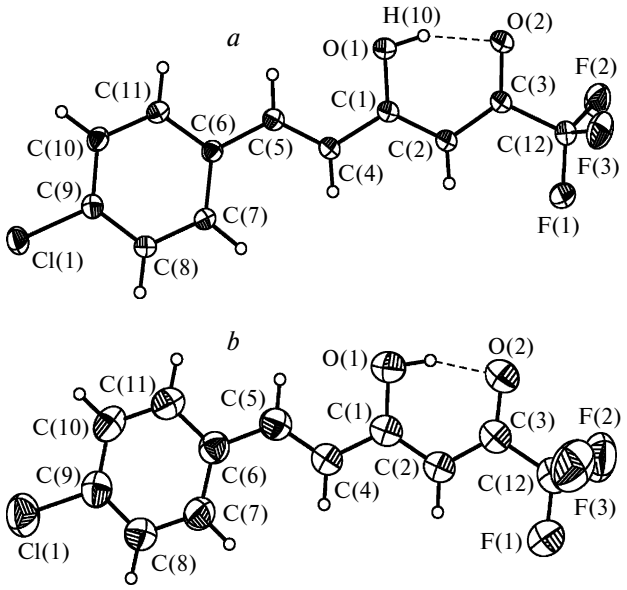

Fig. 1. General view of molecule **2** according to data of X-ray diffraction studies at 120 (*a*) and 300 K (*b*); the atoms are represented by thermal probability ellipsoids (p = 50%).

H-bond in this system leads to a decrease rather than increase in the degree of delocalization of the π-electron density.

A multitemperature X-ray diffraction experiment (120—300 K) showed that, in spite of a slight energy difference between the tautomers, only tautomer **A** characterized by O(1)...O(2) 2.507(2) Å and Q = 0.070 Å (120 K) and 0.063 Å (300 K) (Fig. 1) was observed in the crystal of compound **2** at all temperatures.

Although delocalization of the π-electron density undoubtedly stabilizes the H-bond, in many keto-enols the parameter Q characterizes equalization of the bond lengths due to superposition of tautomers owing to static or dynamic disorder.[12] Structural ordering can be established exclusively based on analysis of the atomic displacement parameters (Hirshfeld test[25]), which, unfortunately, was not performed earlier.[6—11]

Indeed, the quality of an experiment and subsequent refinement can also be assessed from the thermal parameters (atomic displacement parameters). To evaluate them, a test for rigid bonds was proposed.[25] If we denote the root-mean-square displacements of an atom A toward an atom B as $z^2_{A,B}$, the following relation should be valid for any pair of chemically bound atoms A and B:

$$\Delta_{A,B} = z^2_{A,B} - z^2_{B,A} = 0.$$

According to Hirshfeld,[25] the $\Delta_{A,B}$ value for a rigid bond involving a carbon or a heavier atom should not exceed a value of 0.001 Å^2. If this test is not met for a certain fragment of an ordered molecule, the model chosen incorrectly describes the actual electron density dis-

tribution in the crystal and it is highly probable that the molecule under study is disordered.

Ignoring possible disorder in the X-ray diffraction studies of keto-enols led to not only erroneous interpretation of geometric parameters. For instance, in the study of benzoylacetone it was reported that both O—H interactions in the molecule correspond to covalent (shared) bonds, because the $\nabla^2\rho(\mathbf{r})$ values at the (3, −1) critical points of the O...H interactions were negative.[23] However, analysis of the Δ values for the benzoylacetone crystal in the temperature range 8—300 K showed that the Hirshfeld test is met only at 8 K ($\Delta = 7.0 \cdot 10^{-4}$ Å^2 on the average; the maximum Δ value for one of the two C—O bonds is $10 \cdot 10^{-4}$ Å^2).[26] The Δ values obtained for the bonds in the keto-enol fragment at 20 K (neutron diffraction study) and at 143 K (X-ray diffraction study) are respectively $13.6 \cdot 10^{-4}$ and $31.4 \cdot 10^{-4}$ Å^2, (*cf.* $7.8 \cdot 10^{-4}$ and $6.5 \cdot 10^{-4}$ Å^2 for the phenyl ring, see Ref. 26). At 20 K, the maximum Δ value for the keto-enol ring is as large as $40 \cdot 10^{-4}$ Å^2. In spite of so large Δ values for the benzoylacetone crystal at 20 K, the molecule was considered ordered[23,26] and the hydrogen atom position found in the neutron diffraction study at 20 K was used for analysis of the $\rho(\mathbf{r})$ using the data of the X-ray diffraction studies carried out at 8 K.

Actually, the topological parameters of the H-bond in benzoylacetone correspond to a "transition state" of proton transfer, *i.e.* to superposition of two tautomers rather than actual electron density distribution in the keto-enol tautomers.

We observed similar results in the X-ray diffraction study[27] of acetylacetone (**3**) at 110 and 210 K (Fig. 2), which showed that at both temperatures the molecule occupies a special position on the symmetry plane passing through the C(3)—H(3) bond normal to the molecular plane, with the O(1)...O(1a) distance of 2.547(1) and 2.541(2) Å at 110 and 210 K, respectively. In addition to the deformation electron density (DED) maps constructed ignoring the hydrogen atom (see Fig. 2, *b*) an independent confirmation of disorder in molecule **3** is provided by the Δ values of the root-mean-square "counter"-displacements, which are 0.0017 Å^2 (110 K) and 0.0056 Å^2 (210 K) for the O(1)—C(2) and C(2)—C(3) bonds, respectively (see Ref. 27). The barrier to proton transfer in molecule **3** calculated as the energy difference between the structures with C_s and C_{2v} symmetry is 4.45 kcal mol^{-1} (calculated inclusion of zero-point vibrational energy, ZPE).

Interestingly, a multipole refinement performed for two acetylacetone models with the hydrogen atom occupying a special (**3A**) and a general (**3B**) position identically reproduces the character of hydrogen bonds in the ground and transition states according to B3LYP/6-31++G(d,pd) calculations (Fig. 3, Table 1). Both acetylacetone models have similar values of the key

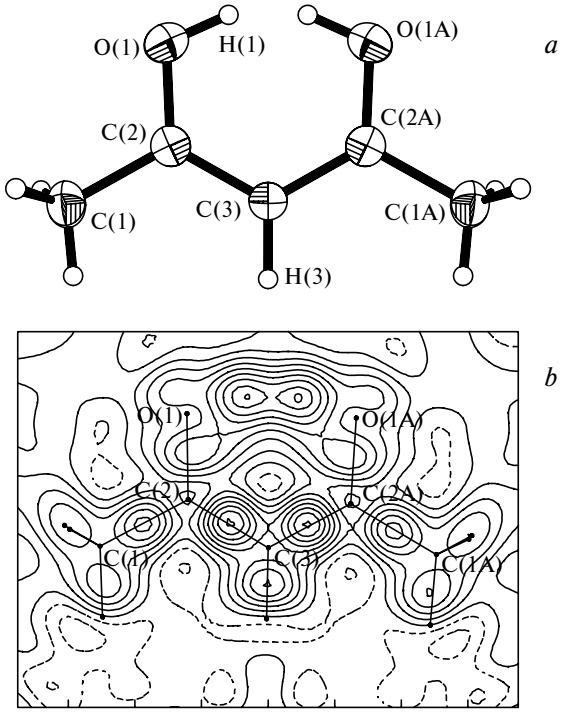

Fig. 2. General view of molecule **3** in the *Pnma* space group at 110 K (*a*); DED maps for **3** (*b*) (promolecule was calculated ignoring the hydrogen atom involved in the H-bond; isolines are drawn with an increment of 0.05 e Å^{-3}).

characteristics of the multipole refinement, namely, the *R*-factors (3.44% and 3.56% for **3A** and **3B**, respectively), residual electron density maps, and topology of the $\rho(\mathbf{r})$

Table 1. Topological characteristics of the electron density in the ground state of the molecule of acetylacetone (**3**) and in the transition state of intramolecular proton transfer according to data of X-ray diffraction study at 110 K and B3LYP/6-31++G(d,p) quantum chemical calculations

Bond	Multipole refinement		B3LYP/6-31++G(d,pd)	
	3A	**3B**	C_s	C_{2v}
H(1)—O(1)*	2.15	1.17	2.10	2.20
	−23.20	−3.32	−40.64	−4.60
O(1)—C(2)	2.43	2.39	2.13	2.33
	−24.33	−28.25	−7.46	−5.58
C(2)—C(3)	1.84	1.84	1.96	2.08
	−16.98	−14.98	−18.34	−14.63
C(2)—C(3A)	1.17		2.20	—
	−3.32		−22.13	
O(1A)—C(2A)			2.52	—
			−2.00	
H(1)...O(1A)	0.22		0.45	—
	3.18		3.29	

* For each bond, listed are the $\rho(\mathbf{r})$ (in e Å^{-3}) and $\nabla^2\rho(\mathbf{r})$ (in e Å^{-5}) values at the (3, −1) critical point.

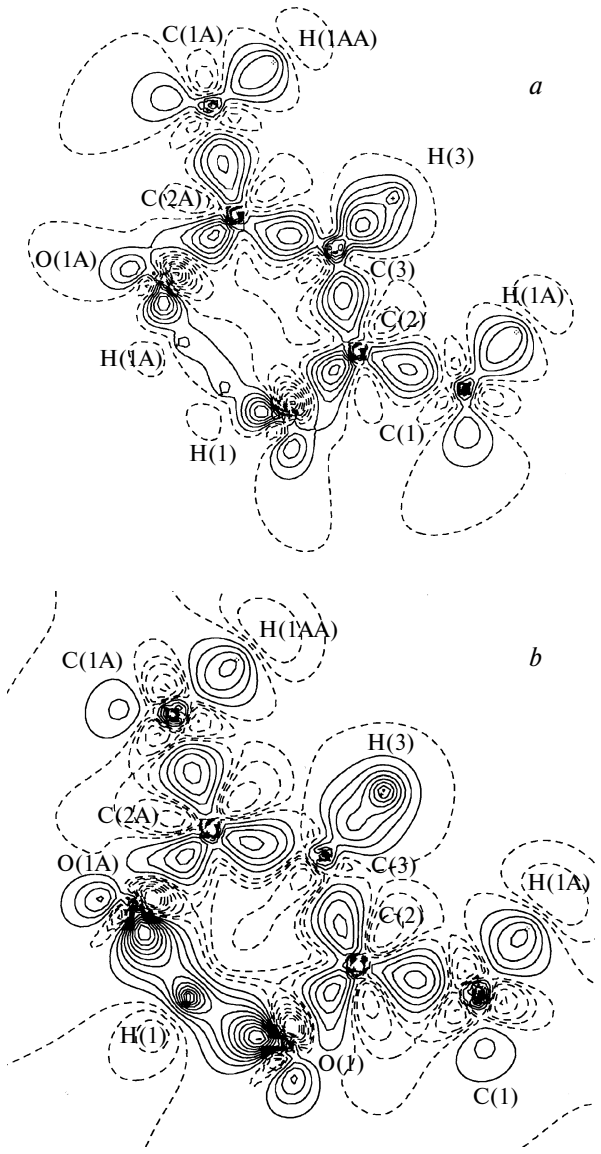

Fig. 3. Static DED maps in the plane of the non-hydrogen atoms in acetylacetone molecule constructed for models **3A** (*a*) and **3B** (*b*) according to the multipole refinement data. Isolines are drawn with an increment of 0.1 e Å^{-3}.

function at the (3, −1) critical points of the C—O and C=C bonds (see Table 1) .

Thus, we obtain quite an unexpected result using the same array of X-ray diffraction data and almost identical structural models (except the position of the H(1) atom). Namely, the topology of the ρ(**r**) function in the region of the H-bond identically describes the ground state and the transition state of proton transfer. It should be noted that if in the ground state the H-bond in molecule **3** corresponds to the intermediate type of the atom-atom interactions (this is similar to molecules **1** and **2**), both O—H interactions in the "hypothetical" transition state correspond to the shared type, which was proposed for benzoylacetone.[23] Since analysis of thermal parameters and geometries of the keto-enol rings in molecules **1** and **2** over a wide temperature range excludes disorder, we can suggest that the shared type of interactions that was revealed for the H-bond in benzoylacetone[23] is an artifact.

The data presented here show that the low barrier to proton transfer along the H-bond line in keto-enols is not always responsible for dynamic disorder in the crystal. For instance, no disorder of the H-bonded ring in compound **1** (barrier to proton transfer is at most 3 kcal mol^{-1} according to B3LYP/6-31G** calculations) was found in the 100—353 K range. At all temperatures, only one, the most energetically favorable, tautomer **1A** (Fig. 4) was realized in the crystal.[12]

Analysis of the intermolecular contacts showed that stabilization of tautomer **A** in the crystal of compound **1** is likely due to the presence of weak intermolecular contacts (*e.g.*, C—H...O) and the stacking interaction of the keto-enol rings (Figs 5 and 6), which lead to substantial increase in the barrier to proton transfer.[12]

However, it is more correctly to analyze the effect of the crystal packing on proton transfer using a system with equivalent keto-enol tautomers, in which (in contrast to acetylacetone) all atoms of the H-bonded ring occupy general positions. The best example is provided by tetraacetylethane (**4**, Fig. 7).[28] According to the data of a neutron diffraction study,[29] at 298 K the molecule in the crystal is located on axis 2 that passes through the midpoint of the C(2)—C(2A) bond and, therefore, one of the keto-enol rings occupies a general position. With allowance for the shorter O...O distance in molecule **4** compared to **3** (2.450 *vs.* 2.547(1) Å, respectively) and for equalization of the bond lengths in the keto-enol ring at 298 K (Q = 0.033),[29] it was of interest to assess the possibility of proton transfer upon raising the temperature.

Indeed, lowering the temperature to 110 K leads to significant changes in the molecular geometry compared

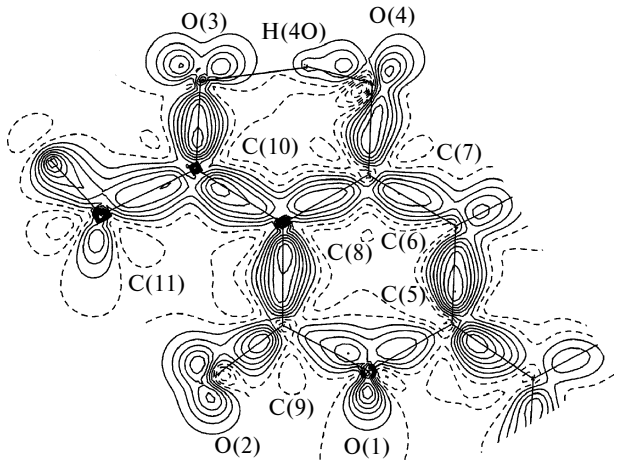

Fig. 4. DED distribution in the region of the keto-enol ring in molecule **1**. Isolines are drawn with an increment of 0.1 e Å^{-3}.

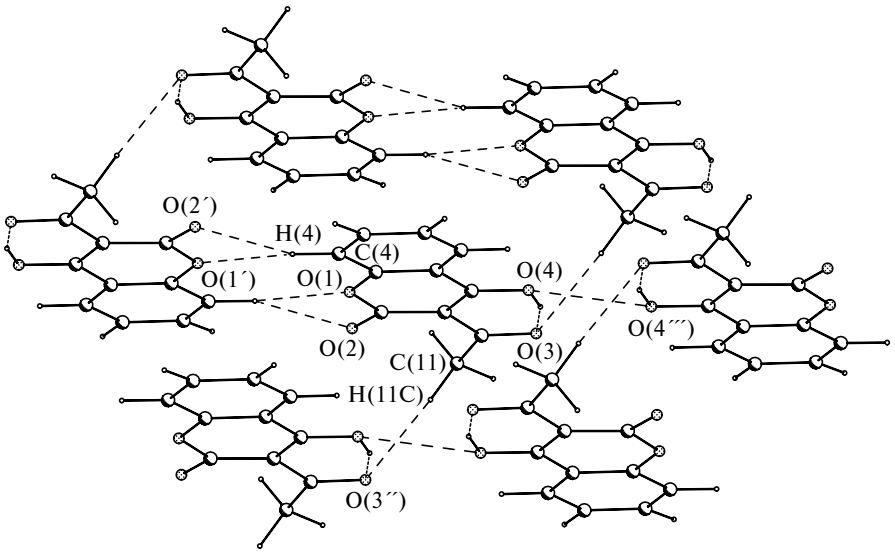

Fig. 5. Formation of C—H...O contacts and the contacts between hydroxyl groups in molecule **1**.

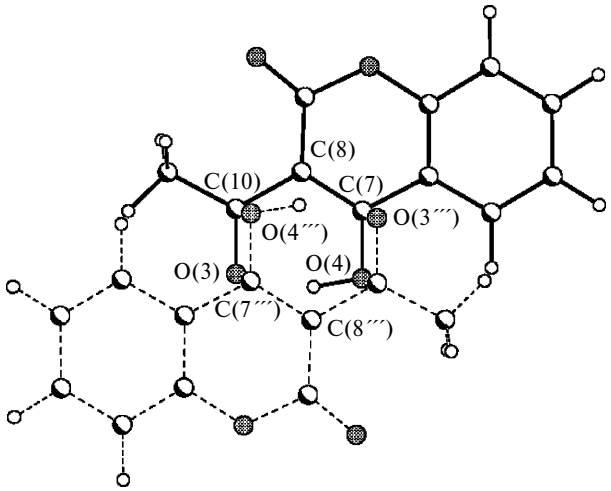

Fig. 6. Interaction between the π-systems of the H-bonded keto-enol rings in the crystal of compound **1**.

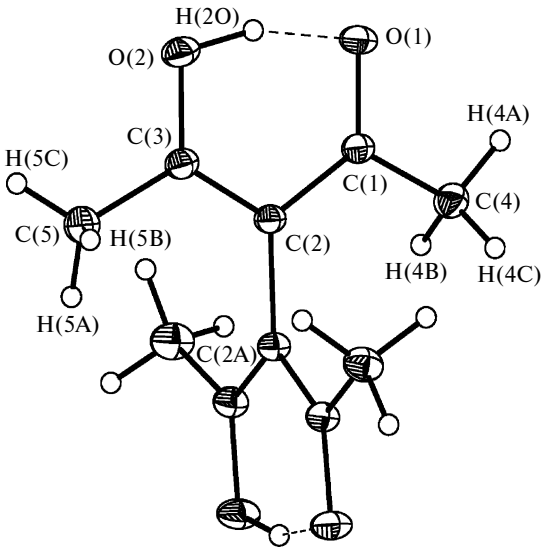

Fig. 7. General view of molecule **4** according to data X-ray diffraction studies at 120 K.

to the data[28] obtained at 298 K. In particular, eqialization of the bond lengths in the six-membered H-bonded ring at 110 K is much less than at 298 K, namely, the Q value increases from 0.033 to 0.085 Å, respectively. Further heating to 350 K leads to almost complete equalization of the bond lengths in the keto-enol ring (Fig. 8).

The observed temperature dependence of the bond lengths in molecule **4** indicates a dynamic disorder, which is confirmed by the analysis of differences between the root-mean-square amplitudes of the "counter"-displacements. For instance, at 110 K the bond lengths in the keto-enol fragment of compound **4** meet the Hirshfeld test[25] (average Δ values are $6.6 \cdot 10^{-4}$ Å^2), whereas raising the temperature to 200 K causes the Δ values to increase to $28.8 \cdot 10^{-4}$ (see Ref. 28). Thus, equalization of the bond lengths in the crystal of compound **4** at 298 K as well as lengthening of the bonds are due to dynamic disorder caused by superposition of the tautomers rather than delocalization of the electron density as a result of the formation of a 3c—4e H-bond.

Taking into account the dynamic character of disorder in molecule **4**, we can assume that the unequivalence of tautomers is due to specific intermolecular contacts that weaken with increasing the temperature, which results in a decrease in the barrier to proton transfer along the H-bond line. Indeed, analysis of the crystal packing showed that the O(2) atom is involved in the formation of the moderate intermolecular contact C—H...O (C(4)—H(4C)...O(2′) (1/2 + x, 1/2 + y, 1+2 − z): H(4C)...O(2′) 2.32 Å, C(4)...O(2′) 3.368(1) Å,

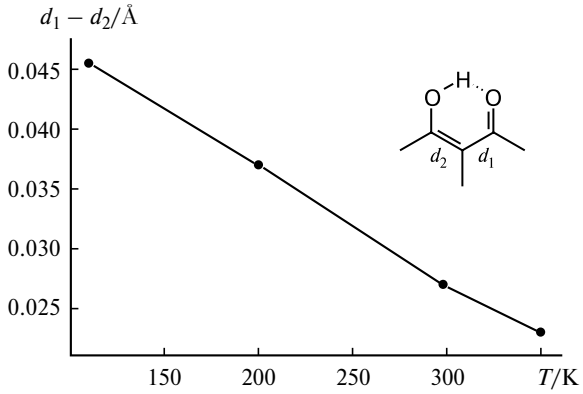

Fig. 8. Bond length differences d_1 and d_2 in the keto-enol ring of molecule **4** plotted *vs.* temperature.

C(4)—H(4C)—O(2′) 163°) (Figs 9 and 10). As the temperature increases, the C...O distance characterizing the strength of the contact changes from 3.369(1) at 110 K to 3.407(2) Å at 298 K.[28]

Analysis of the topological parameters at the (3, −1) critical point of the C(4)—H(4C)...O(2) contact showed that although it belongs to the closed-shell type of interactions ($\rho = 0.095(2)$ e Å^{-3}, $\nabla^2\rho(\mathbf{r}) = 1.34(1)$ e Å^{-5}, $v(\mathbf{r}) = -0.009306$ a.u., $h_e(\mathbf{r}) = 0.002294$ a.u.), the interaction energy calculated from Eq. (4) is 5.8 kcal mol^{-1}. Therefore, this contact in molecule **4** is responsible for the increase in the barrier to proton transfer in the crystal, thus leading to inequivalence of the keto-enol tautomers and to asymmetric O—H...O bond at 110 K. In turn, weakening of this intermolecular interaction with an increase in temperature levels the energy difference between the tautomers, which manifests itself in equalization of the bond lengths in the H-bonded ring.

Table 2. Topological parameters at the (3, −1) critical points of the $\rho(\mathbf{r})$ function and energies of H-bonds in molecules **1—4**

Compound	O...O /Å	$\rho(\mathbf{r})$ /e Å^{-3}	$\nabla^2\rho(\mathbf{r})$ /e Å^{-5}	$-v(\mathbf{r})$ /a.u.	$-E_{cont}$ /kcal mol^{-1}
1	2.442(1)	0.554	5.23	0.1084	34.01
4	2.450(1)	0.517	8.35	0.108	33.88
3	2.507(1)	0.527	1.40	0.0869	27.26
2*	2.547(1)	0.451	3.29	0.0745	23.37

* For compound **2** we present the topological parameters obtained from B3LYP/6-31G** calculations.

Thus, the results we have obtained for a number of keto-enols unambiguously indicate that correct analysis of intramolecular H-bonds is only possible if X-ray diffraction studies involve a detailed analysis of experimental data including the atomic displacement parameters.

Taking into account the fact that the H-bond strength in keto-enols **1—4** is different (O...O distance varies from 2.442(1) Å in **1** to 2.547(1) Å in **2**), it was interesting to compare the changes in the H-bond energies (E_{cont}) of compounds **1—4** estimated from the correlation equation (4)[15] with the changes in the geometric parameters of these molecules (Table 2).

As mentioned above, according to the data of X-ray diffraction studies, the topological parameters at the (3, −1) critical points of the intramolecular H-bonds in compounds **1—4** correspond to the intermediate type of the atom-atom interactions; this is immediately indicated by the negative values of $h_e(\mathbf{r})$ and positive values of $\nabla^2\rho(\mathbf{r})$.

As can be seen, there is no correlation between the electron density values at the (3, −1) critical points of the

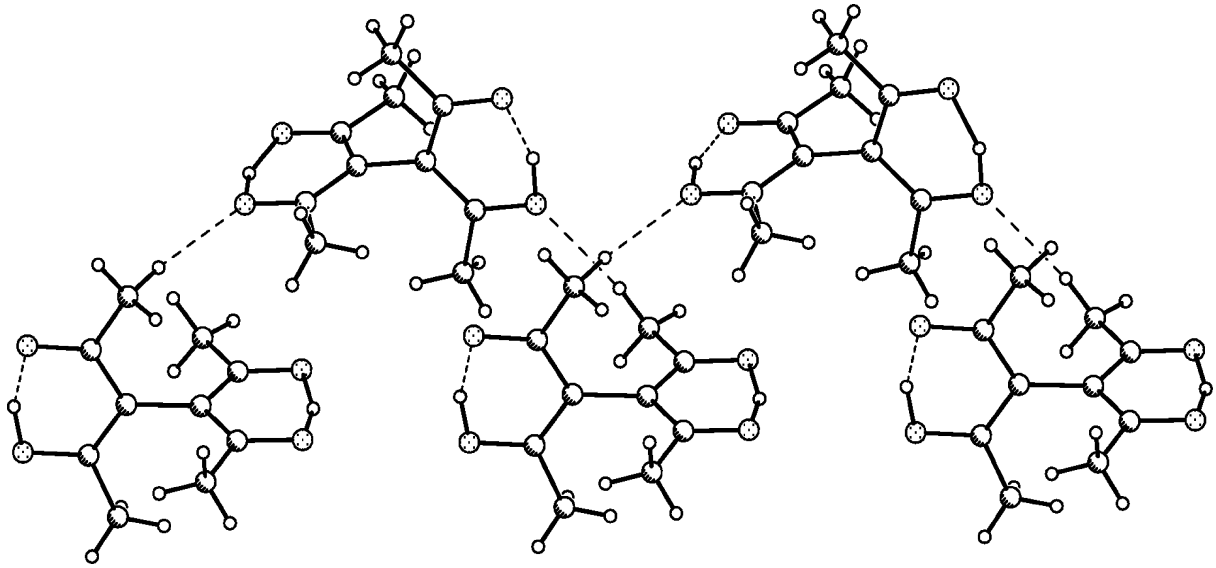

Fig. 9. C—H...O-Bonded chains in the crystal of compound **4**.

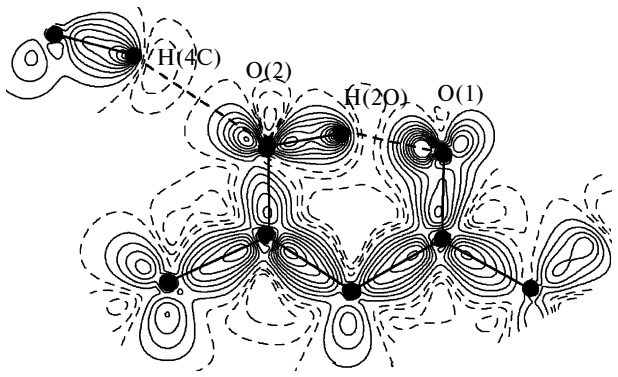

Fig. 10. DED distribution in the plane of the keto-enol ring in the crystal of compound **4**, illustrating the formation of C—H...O contact. The contour lines were drawn with an increment of 0.1 e Å^{-3}.

H-bonds and the O...O distance, whereas the energies calculated using Eq. (4) increase as the O...O distance is shortened.

All the systems with H-bonded rings considered above have a "symmetric" structure of the β-diketone fragment. Because of this, it was interesting to elucidate the character of the atom-atom interactions in the region of the intramolecular H-bond in the systems with chemically inequivalent oxygen atoms (and, hence, with high barriers to proton transfer along the H-bond line). In this work we studied the enol forms of (diphenylphosphoryl)acylacetonitriles **5—8** whose molecules contain a phosphoryl fragment instead of the second carbonyl group.[30—33]

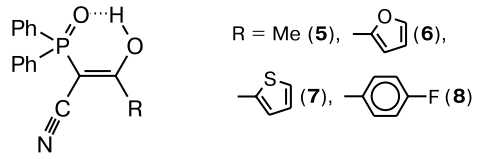

5—8

Interest in these compounds is due to two features. These are strong intramolecular H-bonds both in the crystal[30,33] and in solution[31,32] and an increase in the degree of delocalization of the π-electron density in the H-bonded ring with an increase in the strength of intramolecular H-bonds[30—33] (this is similar to keto-enols).

But unlike keto-enols the barrier to proton transfer in compounds **5—8** is very high[31] and the equilibrium between phosphoryl-enol (**B**)—hydroxy-ylide ketone (**C**) is shifted toward tautomer **B** (Scheme 3).

In all these compounds, the H-bonds are strong. The shortest O...O distance was found in the furyl-containing compound **6** (O(1)...O(2) 2.522—2.528(3) Å), whereas the H-bond in the thiophene derivative **7** is weaker (O(1)...O(2) 2.607(2) Å). Other geometric parameters of the H-bonded ring, namely, the C—O and C=C bond

Scheme 3

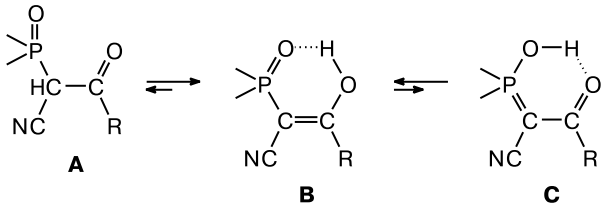

lengths are almost the same despite the variation of the O...O distance.

Compounds **5—8** differ only in substituent at the C(2) atom. Therefore, we can assume that the change in the strength of the H-bond and its decrease in molecule **7** are due to specific stereoelectronic interactions between sulfur atom and hydroxyl group in the H-bonded fragment. However, B3LYP/6-311G** calculations showed that, in contrast to the crystal, the O(1)...O(2) interatomic distances in isolated molecules **5—8** differ only slightly (2.537—2.557 Å) and this distance in compound **7** becomes even some shorter (2.537 Å).

Analysis of the topological characteristics of the ρ(**r**) function in the region of the H-bond showed that these bonds in molecules **5—8** correspond to the intermediate type of the atom-atom interactions (ρ(**r**) = 0.402—0.440 e Å^{-3}, $\nabla^2\rho(\mathbf{r})$ = 3.72—3.85 e Å^{-5}, and $h_e(\mathbf{r})$ = –0.14—0.12 a.u.). Therefore, this type of the atom-atom interactions for strong H-bonds is characteristic of not only low-barrier H-bonds but also of the H-bonds characterized by high barrier to proton transfer. Semiquantitative estimates of the H-bond energies in compounds **5—8** are as follows: 19.45, 20.57, 21.92, and 21.49 kcal mol^{-1}, respectively. Thus, in spite of similar geometric parameters of the H-bonds in molecules **2** and **5—8**, the bonds in the latter group are somewhat weaker.

Analysis of the crystal packing showed that the observed weakening of the H-bond in molecule **7** is due to the intermolecular contact involving the H(2O) atom, which is responsible for the formation of a centrally symmetric dimer (Fig. 11). This intermolecular contact is appreciably weaker than the O—H...O intramolecular bonds in molecules **5—8** (see above). In particular, the O(1)...O(2A) distance is increased to 2.899(3) Å, while the angle at the hydrogen atom is 112° (*cf.* 2.607(3) Å and 159°, respectively, for the intramolecular H-bond).

These intermolecular contacts of the H-bonded rings are not rare in the crystal structures; in particular, an analogous centrally symmetric dimer with the distance between the oxygen atoms of hydroxyl groups of 2.849(1) Å was found in the crystal of compound **1**.[12] It should be noted that in spite of a relatively high energy of this contact (1.75 kcal mol^{-1}), the presence of this contact in the crystal of compound **1** did not lead to signifi-

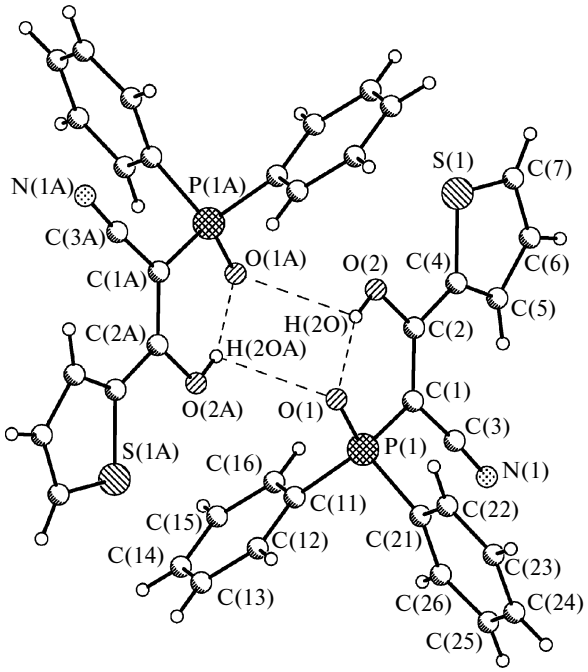

Fig. 11. Dimer formed through O—H...O bonds in the crystal of compound **7**.

cant weakening of the intramolecular H-bond compared to the isolated molecule (see Fig. 5).

Thus, our X-ray diffraction and quantum chemical studies of a number of enol forms of (diphenylphosphoryl)acylacetonitriles **5—8** showed that despite the high barrier to proton transfer the intramolecular H-bonds in these compounds are similar in properties to corresponding intramolecular H-bonds in keto-enols. However, a decrease in the H-bond energy leads to the situation where even weak intermolecular contacts in the crystal affect this energy to a greater extent compared to variation of the substituent at carbon atoms in the H-bonded ring.

Based on this, we can conclude that correlations between the H-bond strength and the electronic effects of substituents in the H-bonded ring obtained in systematic X-ray diffraction studies of strong intramolecular H-bonds involving (strongly) chemically inequivalent proton donor and acceptor can include systematic errors that are due to occurrence of weak competing interactions in crystals with poorly distinguishable effects.

The dependence of the topological parameters at the (3, −1) critical points of the H-bonds (first of all, the $v(\mathbf{r})$ parameter) on the O...O distance makes it possible to employ this approach for comparing the O—H...O bonds in keto-enols with other strong intramolecular H-bonds, such as N—H...O, O—H...N, and N—H...S.

We have chosen and studied a number of compounds characterized by the shortest H-bonds of each type. For instance, the O...N distances (2.481(1) and 2.5238(6) Å) in keto enamines **9** and **10** (Fig. 12) are shorter than in some keto-enols **1—4** (see Table 2) studied earlier[24] even ignoring the difference between the van der Waals radii of O and N atoms.

It should be noted that shortened O...N distances are generally atypical of Schiff bases[2] and occur only in the presence of shortened intramolecular contacts. Such systems were particularly named "sterically modified Schiff bases".

Indeed, as in the "sterically modified Schiff bases" studied earlier,[34—36] the formation of the six-membered H-bonded ring in molecules **9** and **10** [24] leads to realization of shortened intramolecular contacts H...H, namely, H(6)...H(8A) 1.92 Å and H(1)...H(13) 2.01 Å. It should be noted that in (*S*)-1-phenylethylimino-(*S*)-(4-hydroxy[2.2]paracyclophan-5-yl)phenylmethane characterized by one of the shortest O—H...N bonds (O...N 2.465 Å) a similar H...C intramolecular contact between the CH_2 group of the ethylene bridge and the phenyl

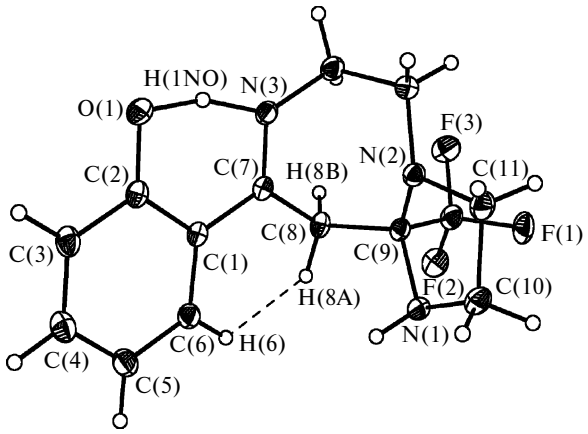

9

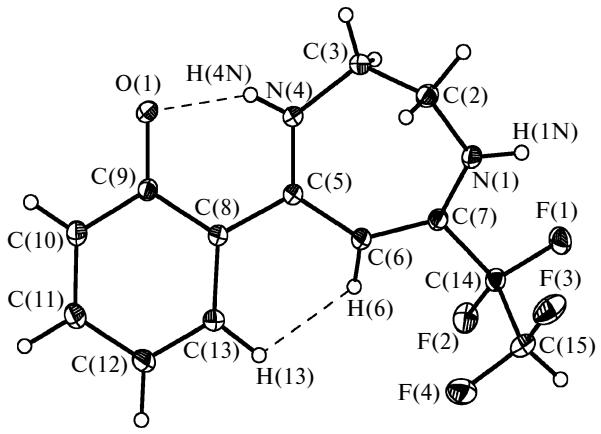

10

Fig. 12. General view of molecules **9** and **10**; the atoms are represented by thermal probability ellipsoids (p = 50%).

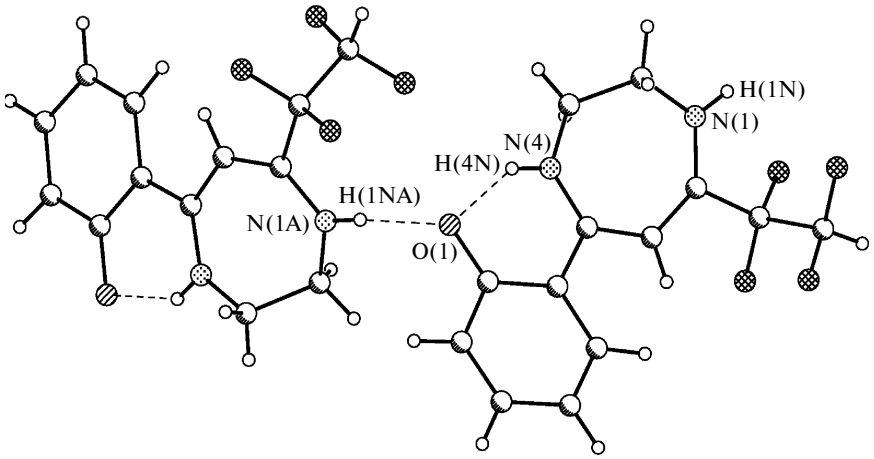

Fig. 13. Fragment of N—H...O-bonded chain in the crystal of compound **10**.

substituent at the nitrogen atom is as long as 2.41 Å (see Ref. 37).

B3LYP/6-311G(d,p) quantum chemical calculations of the imina-enol and keto-amine tautomers **9** and **10** (Scheme 4) showed that their energies differ ony slightly (3.37 and 3.27 kcal mol^{-1}, respectively). For both compounds the energy minimum corresponds to the imina-enol tautomer. Despite the low barrier to proton transfer (at most 3.81 kcal mol^{-1} for **9**), at 110 K the molecules in the crystals **9** and **10** are ordered ($\Delta < 6.6 \cdot 10^{-4}$ Å^2).

Scheme 4

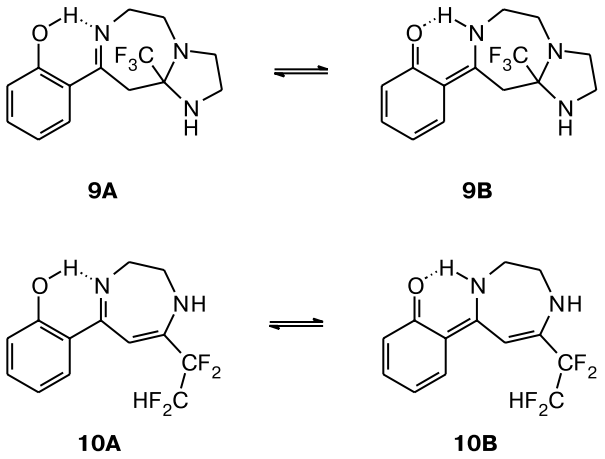

The low barrier to proton transfer provides an explanation for such an appreciable strengthening of the H-bonds in the sterically modified Schiff bases. Indeed, in the transition state of proton transfer the O...N distance is shortened to 2.401 Å, the "cost" of the shortening being only 3 to 5 kcal mol^{-1}. Therefore, the H-bond in keto enamines is readily deformable and is the first to be changes in the sterically overcrowded molecules.

One should also expect a similar effect for keto-enols. This is confirmed by analysis of the published data, according to which the shortest O...O distances (2.374—2.389 Å) occur in the structures with shortened intramolecular contacts (Cambridge Structural Database refcodes DPTBUO, LOJPEF, COPKIB, NMALM, and PINHOJ)*.

In contrast to isolated molecules, the less energetically favorable tautomer **B** is observed in the crystal of compound **10**. A possible reason for stabilization of this tautomer is the formation of an additional, not too strong, intermolecular bond N—H...O (N(1A)...O(1) 2.7705(6) Å), through which the molecules are linked into chains (Fig. 13).

It should be noted that if we are based only on the analysis of geometric parameters, it is logical to assume a large contribution of the zwitterionic form in the case of compound **10**. This is first of all indicated by the C—O bond length equal to 1.3068(5) Å and by the H(4N)—O(1)—H(1NA) bond angle (112°). Taking into account that strong H-bonds are highly directed interactions, that is, the hydrogen atom is directed toward the lone electron pair (LP) of the oxygen or nitrogen atom (Fig. 14), it is logical to assume localization of three LPs on the O(1) atom in molecule **10** (Fig. 15). However, the three-dimensional DED section (Fig. 16) and analysis of the $-\nabla^2\rho(\mathbf{r})$ values at the (3, −3) critical point show that only two LPs lying in plane of the phenyl ring are localized on the O(1) atom. Moreover, the atomic charge of oxygen obtained by integrating the atomic basin O(1) in compound **10** (−0.71 e) is somewhat smaller than the

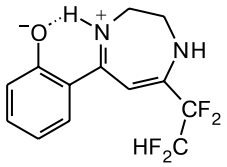

* Refcode is a crystal structure descriptor in the Cambridge Structural Database; all of them are given in accord with Cambridge Crystallographic Database, release 2005.

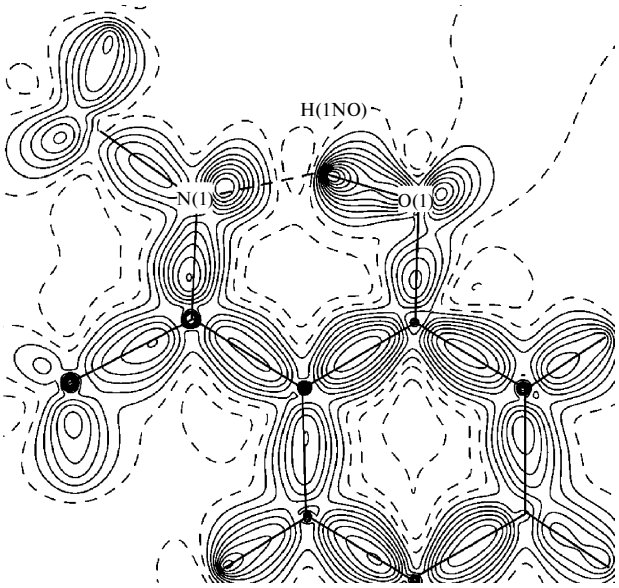

Fig. 14. DED distribution in the plane of the ring formed involving the O—H...N bonds in molecule **9**.

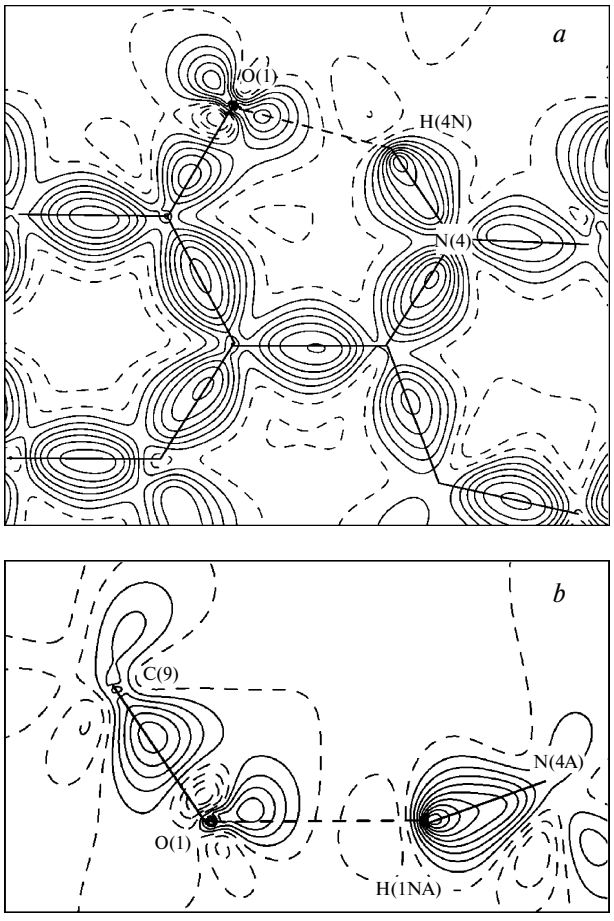

Fig. 15. DED distribution in the plane of the O—H...N-bonded ring in molecule **10** (*a*) and in the plane of the intermolecular H-bond (*b*).

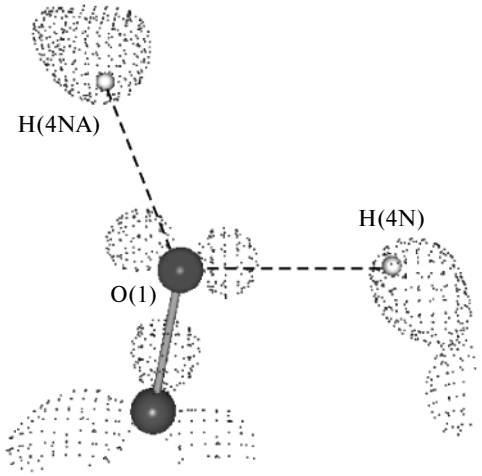

Fig. 16. Three-dimensional DED section in the crystal of compound **10** (shown is the isosurface 0.3 e Å^{-3}).

atomic charge of the carbonyl oxygen, O(2), in compound **2** (−0.87 e).

Search for the (3, −1) critical points of the $\rho(\mathbf{r})$ function in crystals **9** and **10** showed that the forced intramolecular contacts H...H correspond to chemical bonds. The topological parameters at these (3, −1) critical points show that the H...H interactions ($\rho(\mathbf{r})$ = 0.088(4)—0.112(4) e Å^{-3} and $\nabla^2\rho(\mathbf{r})$ = 1.37(1)—1.39(1) e Å^{-5}) are comparable with the moderate C—H...O contacts.[12,15,28,38] Indeed, estimates of the energies of the H...H interactions in molecules **9** and **10** from Eqn. (4) give 2.80 and 3.43 kcal mol^{-1}, respectively.

Analysis of the (3, −1) critical points in the region of the N—H...O and O—H...N bonds in molecules **9** and **10** showed that only the intramolecular H-bonds correspond to the intermediate type of the atom-atom interactions ($h_e(\mathbf{r})$ = −0.011124 and −0.009247 a.u.), whereas the intermolecular H-bond belongs to the closed-shell interactions ($h_e(\mathbf{r})$ = 0.007447 a.u.). Comparison of the topological parameters of the O—H...N and N—H...O bonds with those of the O—H...O bond shows that although the intramolecular H-bonds in compounds **9** and **10** are shorter (with allowance for the difference between the van der Waals radii of O and N atoms), the energies of the latter are lower (see Tables 2 and 3). In turn, comparison of the N—H...O and O—H...N bonds using the published data[39] for the Schiff bases **I—III** shows that they are characterized by higher energies, which can be explained by both larger van der Waals radius and higher diffusivity of the LP of the nitrogen atom.

The decrease in the H-bond energy leads to the change in the interaction type from the intermediate to the closed-shell type. Therefore, it was logical to assume that this type of interactions will also be observed for the N—H...S bonds for which the N...S distance is comparable with the intramolecular interactions considered above (with al-

Table 3. Topological parameters at the (3, −1) critical points of the ρ(**r**) function and energies of hydrogen bonds in compounds **9**, **10**, and **I—III***

Compound	H-bond	O...O /Å	ρ(**r**) /e Å^{-3}	$\nabla^2\rho(\mathbf{r})$ /e Å^{-5}	$-v(\mathbf{r})$ /a.u.	$-E_{cont}$ /kcal mol^{-1}
9	O—H...N (intra)	2.481(1)	0.514	8.1	0.1066	33.44
10	N—H...O (intra)	2.5238(6)	0.357	3.5	0.0550	17.26
10	N—H...O (inter)	2.7705(6)	0.174	4.0	0.0268	8.41
I	O—H...N (intra)*	2.5626(5)	0.43	5.0	0.0758	23.78
II	N—H...O (intra)*	2.6379(5)	0.25	3.1	0.0344	10.79
III	N—H...O (intra)*	2.6688(5)	0.19	3.1	0.0257	8.06

* Topological analysis data taken from Ref. 39.

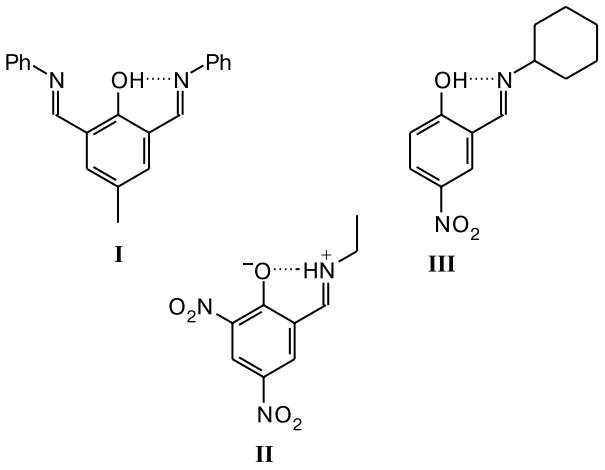

lowance for the difference between the van der Waals radii, that is, 0.34 and 0.65 Å compared to the nitrogen and oxygen atoms).

In order to check this assumption, we carried out an X-ray diffraction and B3LYP/6-311G(d,p) quantum chemical study of compound **11** (Fig. 17). Compound **11** exists in zwitterionic form both in the crystal and in the gas phase (formal positive charge is localized on the N(1) atom and the negative charge is localized on cyanothiamide fragment). The N—H...S bond in this molecule

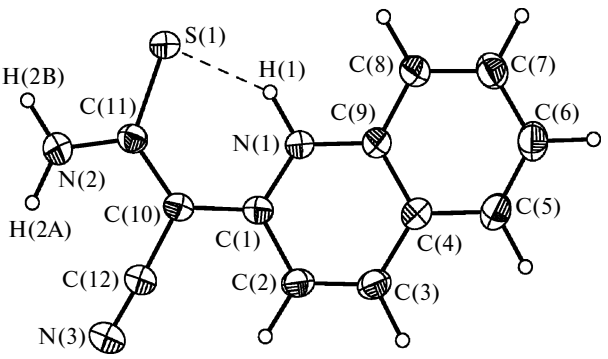

Fig. 17. General view of compound **11**; the atoms are represented by thermal probability ellipsoids (p = 80%).

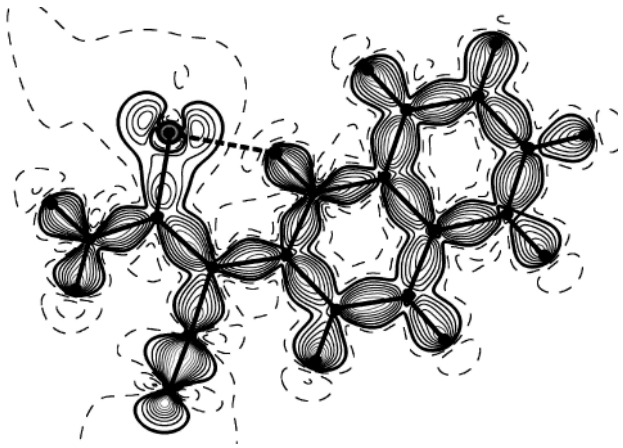

Fig. 18. DED section in the plane of molecule **11**. The isolines are drawn with an increment of 0.1 e Å^{-3}.

belongs to the strongest bonds of this type known to date (N(1)...S(1) 2.9617(5) and 2.991 Å, respectively)[40] (Fig. 18).

Charge calculations performed by integrating the atomic basins in the crystal of compound **11** showed that, although no zwitterionic structure was observed, it is possible to distinguish the regions of positive and negative charges. For instance, the positive charge is mainly local-

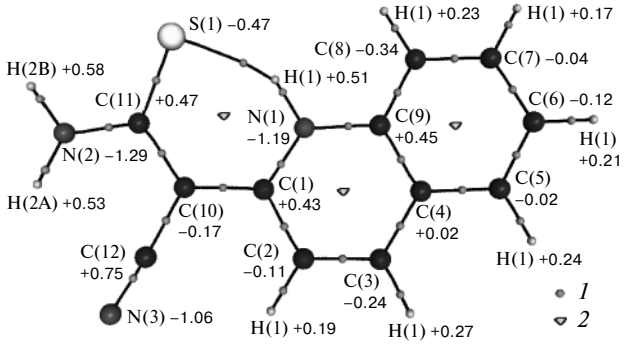

Fig. 19. Molecular graph and charges obtained by integrating the atomic basins in **11**: (3, −1) critical point (*1*) and (3, +1) critical point (*2*).

ized on carbon atoms of the nitrogen-containing ring and the negative charge is mainly localized on the S(1), C(3), C(8), and C(10) atoms and on all nitrogen atoms (Fig. 19).

Analysis of the topological parameters at the (3, −1) critical point of the N—H...S bond showed that in spite of sufficiently low $\rho(\mathbf{r})$ and $\nabla^2\rho(\mathbf{r})$ values (0.23(1) e Å^{-3} and 2.05(2) e Å^{-5}, respectively), the $h_e(\mathbf{r})$ value is negative (−0.0036 and −0.00668 a.u. in the crystal and in isolated molecule, respectively). Hence, as in all the intramolecular H-bonds in compounds **1—10** considered above, here the N—H...S bond corresponds to the intermediate type of the atom-atom interactions. The energy of this bond, estimated from Eqn. (4), is 8.9 kcal mol^{-1}, which is only slightly higher than the corresponding values for the intermolecular bond N—H...O in molecule **10** (see Table 3).

Thus, we can assume that the intermediate type of interactions that was detected in compounds **1—11** is first of all due to the presence of delocalized π-electron system in the H-bonded ring rather than a consequence of high energy of the H-bond.

The topological analysis of the $\rho(\mathbf{r})$ function offers undoubtful advantages for the studies of intramolecular H-bonds. In spite of this the lack of unambiguous methods of estimating the bond energies (see above) makes it impossible to check to which extent the E_{cont} values obtained from the correlation equation (4) correspond to the actual bond strengths.

However, in our X-ray diffraction and quantum chemical studies of phosphorylated thiazolidin-4-ones (**12**) we succeeded not only in studying the reasons for stabilization of particular isomers but also in demonstrating the applicability of the approach described above for estimating the energies of intramolecular H-bonds.[41]

Analysis of the ^{31}P and ^{1}H NMR spectra showed that the shift of the *E*,*Z*-**12**—*Z*,*Z*-**12** equilibrium is governed by the solvent polarity. For instance, in nonpolar solvents, such as C_6D_6, the equilibrium is shifted toward the *E*,*Z*-isomer. On the contrary, in polar protic (CD_3OD) or aprotic bipolar solvents ($CD_3C(O)CD_3$ or DMSO-d_6) the *E*,*Z*-isomer becomes a minor one and the *E*,*Z*/*Z*,*Z* ratio is 23/77 (CD_3OD), 20/80 (DMSO-d_6 : CCl_4 = 2 : 8); and 9/91 (DMSO-d_6 : CCl_4 = 1 : 1) (Scheme 5).

Scheme 5

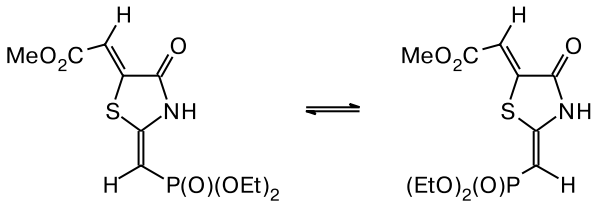

The X-ray diffraction study of the *E*,*Z*- and *Z*,*Z*-isomers showed that they are stabilized through nonvalent contacts (C=O...S and P=O...S), C=O...S contact, and the N—H...O=P hydrogen bond (Fig. 20).

In the crystal of *E*,*Z*-**12**, molecules form centrally symmetric dimers through the intermolecular bonds N—H...O (N(3)...O(1A) 2.877(3) Å), which by analogy with compounds **5—8** considered above should lead to appreciable weakening of this bond. Indeed, B3PW91/6-31G* quantum chemical calculations showed that the N(3)—H(3N)...O(1) bond in isolated molecule *E*,*Z*-**12** is much stronger (N(3)...O(1) 2.745 Å) than in the crystal (2.951(1) Å) or in the isolated dimer formed involving the N—H...O bonds (2.940 Å).

Apparently, the estimate of the energy of the intermolecular H-bond as the difference between the dimer energy and the doubled energy of noninteracting molecules is a rough approximation, because this value

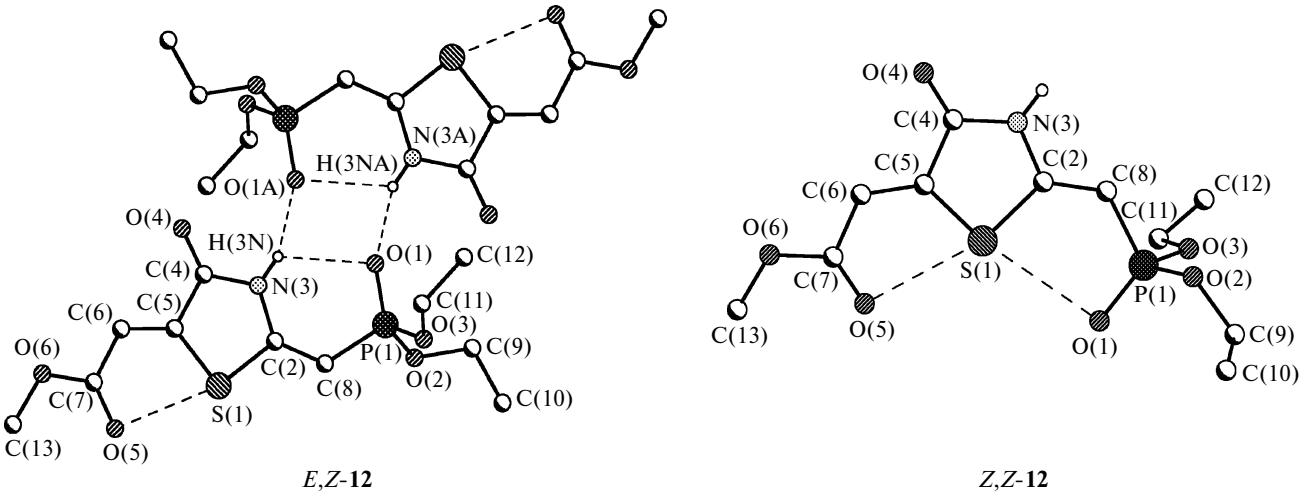

Fig. 20. General view of the *Z*,*Z*-**12** molecule and *E*,*Z*-**12** dimer formed involving N—H...O bonds.

(3.2 kcal mol^{-1} with inclusion of ZPE) also includes the contribution due to the weakening of the intramolecular H-bond.

At the same time the energies of H-bonds in the dimer and monomer can be independently evaluated using the topological analysis of the $\rho(\mathbf{r})$ function. For instance, the energy of intramolecular H-bond calculated from Eqn. (4) is 8.26 kcal mol^{-1} for isolated molecule *E*,*Z*-**12** and decreases to 3.95 kcal mol^{-1} for the dimer. In turn, the energy of the intermolecular H-bond is 6.23 kcal mol^{-1}.

Considering that the energies of the S(1)...O(5) interaction in the dimer and in the isolated molecule are equal (4.26 kcal mol^{-1}) and that in the dimer we can also distinguish the O(1)...O(1A) interaction (2.93 kcal mol^{-1}) similar to those found for compound **1** (see Ref. 12) and for the Schiff base **III** (see Ref. 39), we get that the dimerization energy is 6.67 kcal mol^{-1}. Thus value is in excellent agreement with that obtained as the energy difference between the dimer and monomer (6.40 kcal mol^{-1}). Therefore, our approach provides quite accurate estimates of the H-bond energies and, as can be seen, it is almost twice as large as the value listed above.

Our results also make it possible to explain the equilibrium between isomers observed in solution. Indeed, B3PW91/6-31G* quantum chemical calculations showed that in the isolated state the *E*,*Z*-**12** isomer is energetically more favorable (energy difference between *E*,*Z*-**12** and *Z*,*Z*-**12** is 6.5 kcal mol^{-1} with inclusion of ZPE), which is consistent with NMR data. Since the *E*,*Z*-**12** isomer is mainly stabilized through the H-bond, its weakening can and probably does level the energy difference between the *E*,*Z*-**12** and *Z*,*Z*-**12** isomers.

Thus, our study for the first time made it possible to study the nature of strong intramolecular H-bonds (N—H...O, O—H...O, O—H...N, and N—H...S) and to estimate their energies in relevant molecules. From the experimental data and results of quantum chemical calculations it follows that, in contrast to the geometric parameters, the results of topological analysis of the $\rho(\mathbf{r})$ function allow the energies of the interactions with different proton donors and acceptors to be compared correctly. On the contrary, the values of geometric parameters can include systematic errors, which cannot be revealed without detailed analysis of anisotropic thermal parameters. Additionally, the distance between the proton donor and acceptor (X...Y) is strongly dependent not only on the degree of delocalization of the electron density in the H-bonded ring but also on weak intramolecular interactions, *e.g.*, H...H contacts. Owing to low barrier to proton transfer, the occurrence of such interactions appears to be sufficient for appreciable shortening of the X...Y distance.

This work was carried out with the financial support from the Russian Foundation for Basic Research (Project No. 06-03-32557-a), the Council on Grants at the President of the Russian Federation (Program for the State Support of the Leading Scientific Schools (Grant NSh 1153.2006.3) and young Ph.D. researchers (Grant MK-1054.2005.3)).

References

1. F. N. Keutsch, J. D. Cruzan, and R. J. Saykally, *Chem. Rev.*, 2003, **103**, 2533.
2. P. Gilli and G. Gilli, *J. Mol. Struct.*, 2000, **552**, 1.
3. L. Sobczyk, S. J. Grabowski, and T. M. Krygowski, *Chem. Rev.*, 2005, **105**, 3513.
4. T. Steiner, *Angew. Chem., Int. Ed. Engl.*, 2002, **41**, 48.
5. Yu. V. Zefirov and P. M. Zorkii, *Usp. Khim.*, 1995, **64**, 446 [*Russ. Chem. Rev.*, 1995, **64** (Engl. Transl.)].
6. G. Gilli, F. Bellucci, V. Ferretti, and V. Bertolasi, *J. Am. Chem. Soc.*, 1989, **111**, 1023.
7. P. Gilli, V. Bertolasi, V. Ferretti, and G. Gilli, *J. Am. Chem. Soc.*, 1994, **116**, 909.
8. P. Gilli, V. Bertolasi, V. Ferretti, and G. Gilli, *J. Am. Chem. Soc.*, 2000, **122**, 10405.
9. P. Gilli, V. Bertolasi, L. Pretto, A. Lycka, and G. Gilli, *J. Am. Chem. Soc.*, 2002, **124**, 13554.
10. P. Gilli, V. Bertolasi, L. Pretto, V. Ferretti, and G. Gilli, *J. Am. Chem. Soc.*, 2004, **126**, 3845.
11. P. Gilli, V. Bertolasi, L. Pretto, L. Antonov, and G. Gilli, *J. Am. Chem. Soc.*, 2005, **127**, 4943.
12. K. A. Lyssenko and M. Yu. Antipin, *Izv. Akad. Nauk, Ser. Khim.*, 2001, 400 [*Russ. Chem. Bull., Int. Ed.*, 2001, **50**, 418].
13. R. F. W. Bader, *Atoms in Molecules. A Quantum Theory*, Clarendron Press, Oxford, 1990.
14. Yu. A. Abramov, *Acta Crystallogr.*, 1997, **A53**, 264.
15. E. Espinosa, E. Molins, and C. Lecomte, *Chem. Phys. Lett.*, 1998, **285**, 170.
16. E. Espinosa, I. Alkorta, I. Rozas, J. Elguero, and E. Molins, *Chem. Phys. Lett.*, 2001, **336**, 457.
17. V. G. Tsirelson, *Acta Crystallogr.*, 2002, **B58**, 632.
18. E. A. Zhurova, V. G. Tsirelson, A. I. Stash, M. V. Yakovlev, and A. A. Pinkerton, *J. Chem. Phys.*, 2004, **B108**, 20173.
19. D. A. Kirzhnitts, *Zh. Eksp. Teor. Fiz.*, 1957, **32**, 115 [*J. Exp. Theor. Phys.*, 1957, **32** (Engl. Transl.)].
20. A. A. Korlyukov, K. A. Lyssenko, M. Yu. Antipin, V. N. Kirin, E. A. Chernyshev, and S. P. Knyazev, *Inorg. Chem.*, 2002, **41**, 5043.
21. V. Tsirelson and A. Stash, *Chem. Phys. Lett.*, 2002, **351**, 142.
22. V. Tsirelson and A. Stash, *Acta Crystallogr.*, 2002, **B58**, 780.
23. G. K. H. Madsen, B. B. Iversen, F. K. Larsen, M. Kapon, G. M. Reiser, and F. H. Herbstein, *J. Am. Chem. Soc.*, 1998, **120**, 10040.
24. M. Yu. Antipin and K. A. Lyssenko, *Abstr. Int. Conf. on Hydrogen Bonding (Moscow, Klyaz´ma, October 6—10, 2004)*, Moscow, 2004, L11.
25. F. L. Hirshfeld, *Acta. Crystallogr.*, 1976, **A32**, 239.
26. F. H. Herbstein, B. B. Iversen, M. Kapon, F. K. Larsen, G. K. H. Madsen, and G. M. Reisner, *Acta Crystallogr.*, 1999, **B55**, 767.
27. R. Boese, M. Yu. Antipin, D. Blaeser, and K. A. Lyssenko, *J. Phys. Chem.*, 1998, **B102**, 8654.

28. K. A. Lyssenko, D. V. Lyubetsky, and M. Yu. Antipin, *Mendeleev Commun*., 2003, 60.
29. L. F. Power, K. E. Turner, and F. H. Moore, *J. Cryst. Mol. Struct*., 1975, **5**, 59.
30. M. Yu. Antipin, K. A. Lysenko, Yu. T. Struchkov, I. A. Odinets, O. I. Artyushin, R. M. Kalyanova, T. A. Mastryukova, and M. I. Kabachnik, *Izv. Akad. Nauk, Ser. Khim*., 1995, 1520 [*Russ. Chem. Bull*., 1995, **44**, 1460 (Engl. Transl.)].
31. I. L. Odinets, N. M. Vinogradova, O. I. Artyushin, R. M. Kalyaeva, K. A. Lysenko, P. V. Petrovskii, T. A. Mastryukova, and M. I. Kabachnik, *Izv. Akad. Nauk, Ser. Khim*., 1998, 990 [*Russ. Chem. Bull*., 1998, **47**, 960 (Engl. Transl.)].
32. I. L. Odinets, Ya. A. Vereshchagina, O. I. Artyushin, R. M. Kalyanova, T. A. Mastryukova, E. A. Ishmaeva, G. R. Fattakhova, D. V. Chachkov, and E. G. Yarkova, *Izv. Akad. Nauk, Ser. Khim*., 2003, 611 [*Russ. Chem. Bull., Int. Ed*., 2003, **52**, 638].
33. K. A. Lysenko, D. V. Lyubetskii, M. Yu. Antipin, and I. L. Odinets, *Izv. Akad. Nauk, Ser. Khim*., 2005, 2406 [*Russ. Chem. Bull., Int. Ed*., 2005, **54**, No. 11, 2484].
34. A. Filarowski, T. Glowiaka, and A. Koll, *J. Mol. Struct*., 1999, **484**, 75.
35. A. Filarowski, A. Koll, and T. Glowiak, *Monat. Chem*., 1999, **130**, 1097.
36. A. Filarowski, A. Koll, and T. Glowiak, *J. Chem. Soc., Perkin Trans. 2*, 2002, 835.
37. V. Rozenberg, T. Danilova, E. Sergeeva, E. Vorontsov, Z. Starikova, K. Lyssenko, and Yu. Belokon, *Eur. J. Org. Chem*., 2000, **19**, 3295.
38. K. Wozniak, P. R. Mallinson, G. T. Smith, C. C. Wilson, and E. Grech, *J. Phys. Org. Chem*., 2003, **16**, 764.
39. P. M. Dominiak, E. Grech, G. Barr, S. Teat, P. R. Mallinson, and K. Wozniak, *Chem. Eur. J*., 2003, **9**, 963.
40. K. A. Lyssenko, O. R. Prokopenko, V. N. Nesterov, T. V. Timofeeva, and M. Yu. Antipin, *Mendeleev. Commun*., 2005, 135.
41. V. A. Kozlov, I. L. Odinets, K. A. Lyssenko, S. G. Churusova, S. V. Yarovenko, P. V. Petrovskii, and T. A. Mastryukova, *Heteroatom. Chem*., 2005, **16**, 159.

Received January 15, 2006;
in revised form March 3, 2006